The Seafloor: A Key Factor in Lidar Bottom Detection

Shachak Pe'eri, *Member, IEEE*, James V. Gardner, Larry G. Ward, and John Ru Morrison

***Abstract*—The environmental factors that determine the ability of airborne lidar bathymetry (ALB) to detect the seafloor are not well understood; however, water clarity is often considered the single factor for detection. A comparison of data from two different ALB systems (LADS-MKII and SHOALS-3000) of a small area offshore Gerrish Island, Maine, USA shows a striking correlation (95% overlap) in areas of no bottom detection that is independent of the tide status, the date of collection and the orientation of the survey flight. The laser measurements from the two ALB systems are compared to acoustic measurements of depth, seafloor slope, and backscatter from a Kongsberg EM3002 echosounder. The comparison shows that in water depths deeper than 7 m, there is a close correlation between the ALB detection patterns and bottom features. The study results indicate that lack of bottom detection by ALB does not necessarily indicate that water depths deeper than the surrounding areas have lidar strong bottom detection. No bottom detection in the study area actually reflects a change in bottom characteristics.**

***Index Terms*—Attenuation, laser measurements, light detection and ranging (LIDAR) bathymetry, remote sensing, Seafloor, shallow-water mapping.**

I. Introduction

AIRBORNE lidar bathymetry (ALB) is a bathymetric mapping technique that uses a pulsed laser beam to measure water depths of moderately clear nearshore coastal waters and lakes. ALB survey planning differs from one coastal zone to another because of the environmental factors that affect the success of the lidar survey. The environmental factors are so dominant in ALB that the same survey configuration may, at different times, produce varying bottom detection probabilities. ALB systems consist of an Nd:YAG laser that generates pulses at two wavelengths; the natural wavelength of the Nd:YAG laser at 1064 nm in the infrared, and the frequency doubled wavelength at 532 nm in the green part of the spectrum. The green-wavelength laser pulse is used to provide the main measurement of the water depth [1]. The green-laser pulse interacts with various environmental regions from the time of transmission until the pulse is reflected off the seafloor and received back at the ALB detector.

The main environmental factor groups with which the green-laser pulse interacts can be subdivided into the water surface, the water column, and the seafloor (bottom). The influence of atmosphere on the lidar pulse is very small in comparison to the three other environmental factor groups and can be ignored. Less than 2% of the green-laser pulse is reflected back into the air from the surface of a body of water and sensed by the receiver as the "surface return" [2]. The remaining portion of the green-laser pulse is refracted into the water column where scattering from entrained microscopic particulates causes it to spread into a cone of continuously increasing angle. A small fraction of the transmitted energy in the water column, whose magnitude exponentially decreases with depth, becomes incident upon the bottom with a lateral extent that depends on water clarity and single scattering albedo. A portion of the energy incident on the bottom (typically 4–15% depending on the bottom composition) is diffusely reflected back into the water column. Scattering and absorption attenuate and stretch the reflected energy as it passes back to the surface, where much of the remainder is refracted into the air. The airborne optical receiver can then intercept a fraction of this returning energy (whose magnitude depends on the aircraft altitude, water depth and clarity, receiver aperture, and receiver field of view) and interpret it as the "bottom return" [2].

The parameters of each of the three main environmenta factor groups vary with time for a given location and each parameter's rate of change differs from one another. The water surface is mainly affected by capillary and gravity waves, white caps, and sun glint (which depends on the relative angle of the lidar to the sun with respect to the water surface) [3]–[5]. The rate of change of water surface factors can vary from seconds to minutes. The dominant factors in the water column are colored dissolved organic matter and organic and inorganic suspended particulates [6]–[9]. These factors are sometimes combined and called water clarity. The rate of change of water column factors ranges from seconds to months. The dominant factors of the seafloor that influence the laser pulse are the bottom reflectance at the laser wavelength, bottom slope, roughness, the presence of vegetation, and indirectly the presence of macrobenthic animals (such as, worms) [5]–[7], [10]–[15]. The rate of change of seafloor factors can vary from hours to months. Only a few studies have investigated the contribution of the seafloor to lidar performance [7]–[12].

The conventional assumption is that the dominant environmental factors that influence the ability of a lidar to detect

Manuscript received September 22, 2009; revised April 2, 2010 and July 1, 2010; accepted August 5, 2010. Date of publication October 11, 2010; date of current version February 25, 2011. This work was funded by the University of New Hampshire Tyco Fellowship for Ocean Mapping and UNH/NOAA Joint Hydrographic Center Grant NA05NOS4001153.

S. Pe'eri, J. V. Gardner, and L. G. Ward are with the Center for Coastal and Ocean Mapping (CCOM), University of New Hampshire, Durham, NH 03824 USA (e-mail: shachak@ccom.unh.edu).

J. R. Morrison was with the Center for Coastal and Ocean Mapping (CCOM), University of New Hampshire, Durham, NH 03824 USA. He is now with the Northeastern Regional Association of Coastal Ocean Observing Systems (NERACOOS), Rye, NH 03870 USA.

Digital Object Identifier 10.1109/TGRS.2010.2070875

the bottom are the water column group (i.e., water clarity) (e.g., [1], [16], and [17]). As a rule of thumb, bottom detection using commercial ALB systems ranges up to 2–3 times the Secchi depth. This assessment is quantified by a physical optical parameter, the diffuse attenuation coefficient (K) at the green-laser wavelength [2]. Lidar surveys are accordingly planned to operate under the most ideal water clarity conditions. The planning includes consideration of night flights for reduced background noise and tidal phases and weather conditions to minimize suspended particulates in the water.

This paper presents field observations and a theoretical model of the nature of the environmental factor groups and their influence on the ALB measurements. Observations from two different ALB systems are compared to an acoustic survey conducted with a high-resolution multibeam echosounder. The objective of this comparison is to quantify the influence of the seafloor environmental factor on ALB bottom detection and investigate the assumption that an area with no bottom detection within a data set is deeper than the surrounding bottom-detected areas by laser measurements.

II. Lidar Equation

Data from two types of ALB systems were used in this study: a LADS MK-II and a SHOALS-3000. Both systems operate with an Nd:YAG laser that transmits pulses at two wavelengths (532 and 1064 nm) with a pulse repetition frequency of 900 Hz for the LADS MK-II and 3000 Hz for the SHOALS-3000. The LADS MK-II survey design operates with a vertically fixed 1064-nm infrared (IR) beam and a rectangular survey pattern for the 532-nm green beam with a maximum off-nadir angle of 15° [18], [19]. The survey scan patterns of the green and the IR beams of the SHOALS-3000 system form a section of a circular arc, where the beams are maintained at a constant 20° off-nadir angle [1]. The ocean optical pathways for both systems are the same: the green-laser pulse first encounters the water surface, then passes through the water, interacts with the bottom and is reflected back through the water column, and finally through the water/air interface to the sensor. The travel path of the green-laser pulse is twice through the air/water interface, twice through the water column and once reflected from the seafloor.

Guenther [2] formulates these environmental factors into a lidar equation. In his equation, the received pulse energy E_R from a transmitted pulse of energy E_T with an effective slant range (water to bottom) of R_S and with a solid angle ratio of the receiver to the effective bottom-returning energy above the air/water interface Ω_R/Ω_B is

$$E_R = E_T \eta L \rho \frac{\Omega_R}{\Omega_B} F e^{-2KR_s} \tag{1}$$

where η is the optical loss factor (transmitter and receiver); ρ is bottom reflectivity; L is the environmental loss factor; and F is the loss factor due to insufficient receiver field of view. Although modifications to the lidar equation have been suggested [20], [21], the development of the newer equations follows the same basic logic.

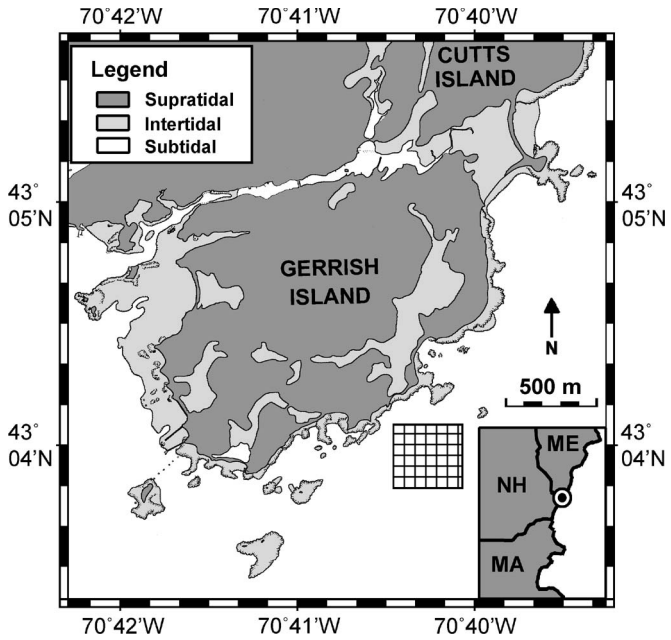

Fig. 1. Location map of the study area (gridded area) offshore Gerrish Island, Maine, USA. All areas below Mean Lower Low Water (MLLW) are referred to as subtidal, areas between MLLW and Mean High Water (MHW) are referred to as intertidal; and all areas above MHW are referred to as supratidal.

Lidar performance has been evaluated for more than 20 years in the context of the water column influence on the lidar measurement. The main reason for this was to maximize the penetration through the water column using the laser pulse [2], [18], [22], [23]. Accordingly, ALB system design focused on the receiver field-of-view for successfully measuring the diffuse attenuation [2], [24]. This is reasonable, considering that the first environmental factor group that strongly influences the lidar is the water column group. Research targeted to the seafloor group began in recent years. The main focus is on the potential use of ALB for seafloor characterization and the capabilities to classify the seafloor using the lidar waveforms [9], [11], [13], [21], [25]. To the knowledge of the authors, these studies have all focused on the use of ALB products and did not investigate the lidar performance and its relation to the seafloor environmental factors.

III. Observations

A. Gerrish Island Data Set Project

Two ALB surveys were conducted in 2005 offshore Gerrish Island, Maine, USA in the western Gulf of Maine (Fig. 1). A LADS MK-II survey was conducted on August 17–18, 2005 and a SHOALS-3000 survey was conducted on September 30 and October 3, 2005. Water level changes due to tide during the surveys reached 1.4 m during the LADS survey and 0.7 m during the SHOALS survey. The LADS survey was conducted according to National Oceanic and Atmospheric Administration (NOAA) survey standards that require a 3 m × 3 m spot spacing with a 200% overlap. The SHOALS survey was conducted according to U.S. Army Corps of Engineers (USACE) survey standards that require a 4 m × 4 m spot

spacing with a 100% overlap. Both surveys were processed by the respective surveying groups (NOAA and USACE). The data used in this study are the edited location and depth information (X, Y, Z) of the laser measurements.

Acoustic measurements from a 300-kHz Kongsberg EM3002 multibeam echosounder, video and bottom samples were used as a reference data set for the study. The acoustic data were collected on June 6–15, 2006 by the Center for Coastal and Ocean Mapping (CCOM), University of New Hampshire (UNH). A 1-m resolution digital terrain model (DTM) and a slope map of the bathymetry were produced from the acoustic data, as well as an acoustic backscatter mosaic of the seafloor. The acoustic survey was planned and conducted based on the coverage and the bottom detection patterns of both lidar surveys. Although the acoustic survey occurred 9–10 months after the lidar surveys, temporal horizontal changes of the seafloor in the study area are small (sub-meter) relative to the lidar horizontal survey resolution (order of meters to tens of meters) over this time period.

Observations from the UNH Coastal Observing Center's monitoring of the western Gulf of Maine at station WB1, approximately 1.5 km to the southeast (43.0546° N, 70.6581° W, water depth ∼22 m), were used for evaluating the optical properties of the water at the time of the lidar survey. Profiles of the downwelling irradiance, $E_d(\lambda)$, and upwelling radiance, $L_u(\lambda)$ were measured using a hyperspectral profiling radiometer (Hyperpro-II, Satlantic Inc.) with associated deck reference. The sensors measured light intensity in 137 wavebands with approximately 3-nm spacing from 350 to 800 nm. The downwelling diffuse attenuation coefficient, $K_d(\lambda)$, and upwelling radiance attenuation, $K_{Lu}(\lambda)$, were calculated at each depth as the slope of the log transformed light levels with a depth window of 5 m around the measurement depth.

B. Bottom Detection and Lack of Bottom Detection

Visual inspection of the lidar surveys shows a comparable performance in bottom detection. Good bottom detection was acquired over much of the region by both systems although there are areas of no bottom detection from both systems. In fact, the areas of no bottom detection are almost identical in both surveys. The bottom detection by both systems occurred within the 3–14 m range of water depths, whereas areas with no bottom detection ranged within similar water depths from 5 to 13 m. The high-resolution multibeam survey over the area provides an independent measure of water depth and shows that the areas of bottom detection are flat, relatively featureless seafloor, and tops of outcropping rocks. The multibeam survey shows that the areas of no bottom detection are the sides of the outcrops and bottom features with vertical variance. Finally, the backscatter values from the multibeam survey show different values than the areas with strong bottom detection.

A seafloor area of 0.5 km × 0.5 km located about 1 km southeast of the Gerrish Island, Maine, USA (Fig. 2) was chosen for a detailed analysis. Water depths in this area range from 3 to 15 m. Information on bottom samples collected before the study was not available and according to the NOAA charts this area

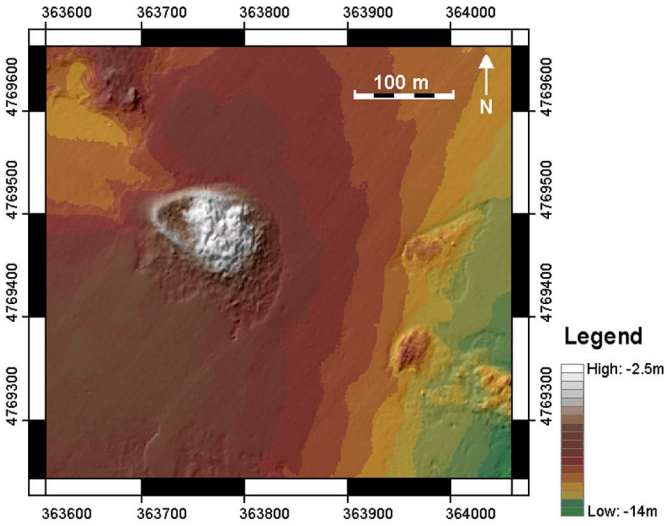

Fig. 2. Color-coded shaded relief multibeam bathymetry map of the study area. The depth values are relative to the MLLW.

is considered rocky. Bottom samples collected for this study as ground truth show that the seafloor in this area is composed of rocky and sandy regions. Comparison of neighboring lines in each of the surveys shows that the spatial boundaries of the patterns are almost identical. The spatial boundaries were delineated based on the laser measurements density (minimum of 5 laser measurements for a 10 m × 10 m area). Fig. 3 presents the detection patterns of the ALB survey lines for the SHOALS-3000 survey [Fig. 3(a)] and the LADS-MKII [Fig. 3(b)] survey. The detection patterns were separated into two area groups based on their bathymetry and will be described in detail in the next section.

The correlation in bottom detection success is independent of the time of collection; the spatial boundaries of the detection patterns are similar and independent of the sun angle, tide status, and the water conditions. The spatial boundaries of detection patterns were digitized and stored as polygon shapefiles. The overlaps between the two lidar surveys, converted to grid cells of the polygons, were calculated using a correlation matrix that resulted in a 95% correlation between surveys (Table I). Because of this large overlap and the similarity in detection from each lidar system, an average detection pattern of the two lidar systems was generated. The cause of the lack of bottom detection by both systems is not clear from the lidar survey and information from a multibeam echosounder survey over the study area was used as a reference surface.

IV. Observations Physical Properties

A. Bathymetry

The lack of bottom detection in ALB is usually attributed to a longer path of the laser pulse through the water column that is related directly to the local bathymetry. The level of optical interactions that the laser pulse experiences is a function of the path traversed through the water column. Consequently, the deeper the water depth, the greater the water column interactions and hence more attenuation of energy from the

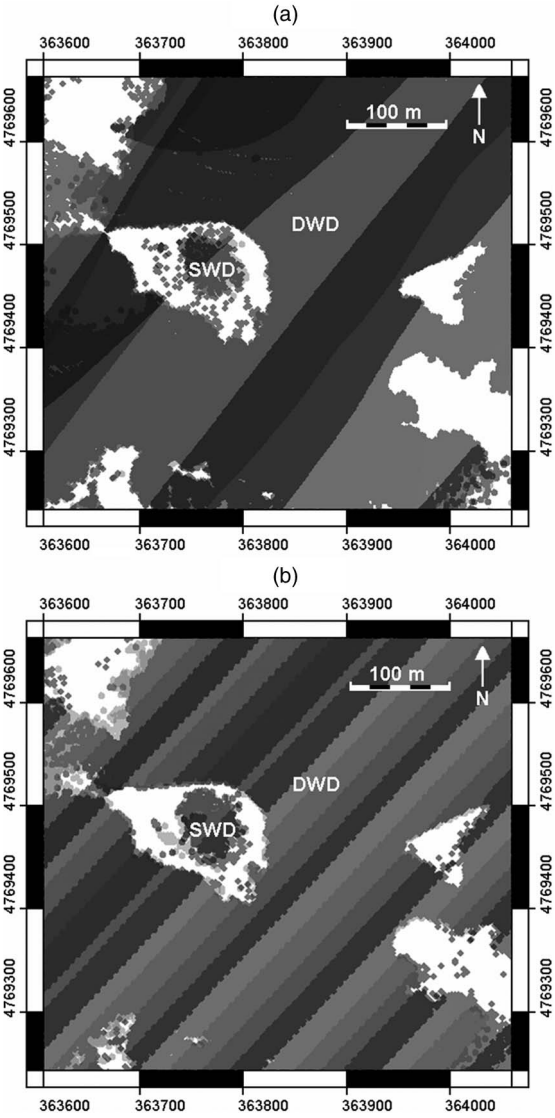

Fig. 3. Detection patterns of the laser measurements collected by: (a) SHOALS-3000; and (b) LADS MK-II ALB systems. The laser measurements are color-coded with 50% transparency for each survey line and are plotted in 19N UTM WGS-84 coordinate system. The bathymetry area groups are: DWD- deep-water detection areas; SWD- shallow-water detection area; White: lack-of-detection areas.

TABLE I
CORRELATION MATRIX OF THE DETECTION (DEEP-WATER DETECTION AND SHALLOW-WATER DETECTION AREAS) AND LACK-OF-DETECTION AREAS FROM BOTH LADS AND SHOALS SURVEYS

LADS \ SHOALS	Detection	Lack-of-detection	Sum
Detection	162982	8292	171274
Lack-of-detection	1799	25617	27416
Sum	164781	33909	198690

transmitted laser pulse before it returns to the lidar detector. The frequency histograms of the gridded pixels for both polygons (lack-of-detection or detection) were plotted as a function of water depth at a 0.5-m bin resolution. The frequency histograms indicate two separate subgroups that occur in the area of bottom detection (2.5–7.0 m and 7.5–14.0 m) (Fig. 4).

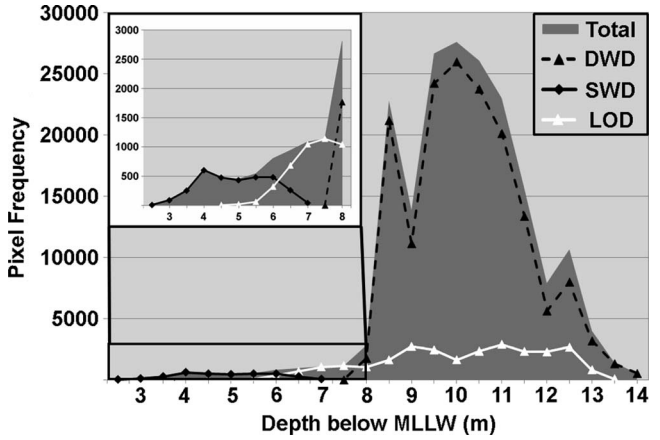

Fig. 4. Histogram of pixel frequency as a function of bathymetry (0.5 m bins). DWD- deep-water detection areas; SWD-shallow-water detection area; LOD—lack-of-detection areas.

Originally, the study focused only on the water depths that range from 8 to 13 m that contain the lack-of-detection areas (bottom right in Fig. 3). After observing the frequency histogram results (total, lack-of-detection, and detection) over a broader depth range that includes shallow waters, the study area and the depth range were expanded. Although the number of the pixels with bottom detection in water depths that range from 3 to 8 m increases with depth, no successful bottom detection was made between 7 to 7.5 m. The bottom-detection area polygons were divided into two groups based on this depth range [Fig. 3(a) and (b)]. The groups were named as follows: deep-water detection areas and shallow-water detection area. The results in Fig. 4 show that the lack-of-detection areas and deep-water detection areas share the same depth range. This indicates that in water depths that range from 7 to 14 m, the bottom detection is not only dependent on the distance the lidar returns travel within the water column, but also must depend on other environmental factors. The number of pixels that overlap in depth (6–7 m) between lack-of-detection areas and the shallow-water detection area is small (∼4,000) compared to that in the deep-water detection areas (∼182 000). Therefore, the 7-m water depth can be regarded as a boundary between the shallow-water detection and deep-water detection.

The depth range limit defined here represents the shallow water depth range where ALB bottom detection is successfully independent from the seafloor characteristics. The depth-range limit value (7 m) depends on the water clarity (average diffuse attenuation value was 0.2 m^{-1}) during the August-October 2005 surveys. However, areas in water deeper than 7 m where the lidar measurements were not able to detect the bottom are shallower than their surrounding areas where bottom was successfully detected. It is highly unlikely that the lack of bottom detection was caused by water column environmental factors, but rather it was caused by a seafloor environmental factor. Examination of the multibeam bathymetry verified that the area of lack of detection was shallower than the deep-water detection (especially in the area at the center left of Fig. 3). This implies again that the seafloor environmental factor was the contributing factor. ALB lack of bottom detection due to suspended sediment in the water column is also unlikely

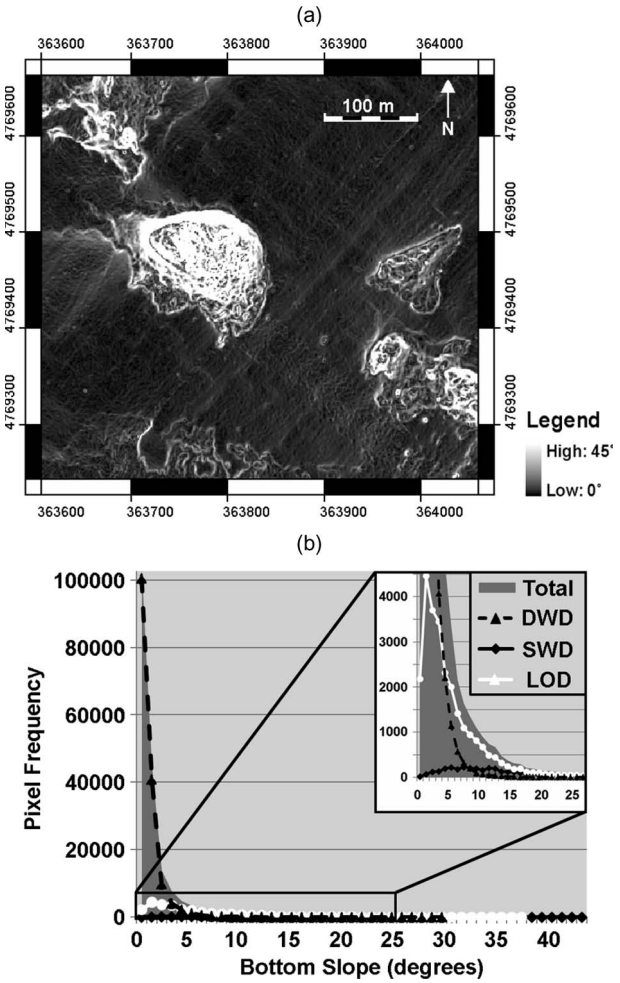

Fig. 5. (a) Bottom slope image of the study area calculated over a 1-m distance produced from the acoustic multibeam bathymetry. (b) Histogram of pixel frequency as a function of absolute slope (1° bins). DWD- deep-water detection areas; SWD- shallow-water detection area; LOD—lack-of-detection areas.

because the tidal currents in the area were strong enough to transport fine-grained particulates out of the area in a relatively short time period.

B. Slope

The first component that is an indicator of the seafloor environmental factor group is the slope of an area. The slope is a derivative of the bathymetry and can be used to describe the spatial vertical variability of the seafloor and the angle of incidence of the lidar-pulse with the seafloor. The water surface footprint of the laser pulse from both lidar systems is about 2 m in diameter. The laser pulse expands in the water column as a cone due to scattering. For most operating conditions, the 3-db (half energy) beam diameter at the seafloor will expand an additional 10–30% of the depth; for extreme conditions near extinction, the 3-db beam diameter can be as large as half the depth [1].

A 1-m grid slope map was produced from the acoustic multibeam bathymetry (Fig. 2). A maximum slope was determined by from the 1-m grid. Also, the pixel frequency in both the lack-of-detection and in the bottom-detection areas is plotted

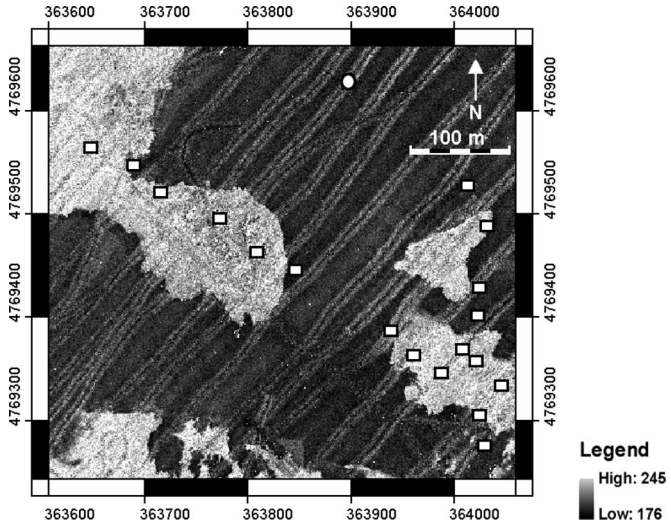

Fig. 6. Acoustic backscatter map of the study area. White circle—bottom sample location at the time of the acoustic survey in 2005; white rectangles—bottom samples and underwater video locations in 2008.

as a function of slope bins [1° bins; Fig. 5(b)]. An analysis of the slope-range distribution shows different distribution functions for each group that overlap in slope values. 95% of the laser measurements in the deep-water detection areas occur on slopes 0°–3°, whereas lack-of-detection areas occur on slopes of 0°–13°, and shallow-water detection areas occur on slopes that range from 0° to 23°. These results show that there is no correlation between the slope of the seafloor and the ability of the lidar to detect the bottom.

C. Acoustic Backscatter

A second component that is an indicator of the seafloor environmental factor group is the intensity values of the 300-kHz sonar returns that are used for seafloor characterization [26]. At a frequency of 300 kHz, assuming all else is held constant, the acoustic backscatter is an observation of the acoustic properties of the seafloor and not of the optical properties of the water column. However, the correlation between lidar bottom-detection pattern and the backscatter patterns (changes in the acoustic properties) suggests a dependence of the seafloor physical characteristics and the lidar measurements.

The multibeam echosounder backscatter shows a good correlation between the acoustic properties of the seafloor (backscatter intensity) and the areas lacking bottom detection by the lidar surveys. Fig. 6 also suggests that the shallow-water detection area and lack-of-detection areas have the same seafloor characteristics, whereas the seafloor characteristics (at 300 kHz) of deep-water detection areas are different. Bottom samples and underwater video that were collected as additional ground truth data for the study confirm these results.

V. Discussion

Comparison of the results of the two ALB surveys and multibeam survey shows that the lidar deep-water detection areas and the lack-of-detection areas are correlated with the seafloor environmental factor groups (the acoustic properties of the

seafloor). Two possible explanations are proposed; geologic-seafloor composition or marine vegetation, both of which affect the ALB's ability to detect the seafloor. Two bottom samples were taken in the low-backscatter areas during the acoustic survey (one of the bottom samples was in the study area; Fig. 6). The two samples are olive gray fine-grain sand (hue 5Y, value/saturation 3/2). Several attempts to sample the high backscatter-value areas failed. The assumption made was that the seafloor in the high-backscatter areas is most likely rocky bottom as suggested by the failure of the grab sampler, the high acoustic backscatter, and the steep slopes. However, the option of a vegetated bottom (regardless of the bottom composition) cannot be ruled out. In order to resolve this uncertainty, additional bottom samples and underwater video imagery were collected at 17 stations three years after the lidar surveys. All bottom samples in the low backscatter-value areas are olive gray fine-grain sand (hue 5Y, value/saturation 3/2). The video imagery shows no underwater vegetation present. Bottom sampling in high backscatter-value areas failed to recover samples, although few caught pebbles or vegetation. The video imagery shows that no sand is present and the areas contain pebbles, cobbles, rocky outcrop, and vegetation.

1) *Geologic seafloorcomposition:* The first explanation is that the lack of bottom detection correlates with areas of rocky seafloor. A simplified case of an ALB pulse is when the laser pulse interacts with a flat sandy bottom to produce a single interaction. This interaction and loss of energy will be the bottom reflectivity parameter ρ in the lidar equation. However, in a case where the laser pulse interacts with a steep-sloped rocky area (with the same reflectance values as in the first case), multiple interactions may occur as energy is reflected off facets to other facets in the steep-sloped bottom. This would occur at a microscale (centimeter and smaller level) and should not be confused with the DTM slope (meter level) mentioned in the previous section. In each interaction of a laser pulse with the seafloor, the returned energy is reduced by the bottom reflectance that reduces the amount of energy returning to the ALB detector. Additional reduction of the laser-pulse energy will be caused by the angle of incidence between the laser pulse and the seafloor slope. This will require modification of the bottom reflectivity ρ in the lidar equation and the addition of a correction such as the Minnaert Correction [27], [28]

$$\rho_H = \rho_T \left(\frac{1}{\cos i} \right)^k \tag{2}$$

where ρ_H is the reflectance observed for a horizontal surface, ρ_T is the reflectance observed over a sloped terrain, i is the incident angle on a pixel relative to the normal and k is computed empirically.

2) *Vegetation:* The second explanation for the lack of bottom detection is that it is related to the presence of aquatic vegetation on the seafloor. A simplified case is when the laser pulse interacts with a flat sandy nonvegetated bottom to produce a single interaction. In this case, almost all the energy is reflected back from the bottom at the same wavelength at which it was transmitted (elastic scattering). However, in a vegetated bottom scenario, the bottom reflectivity ρ needs to be modified so that each interaction through the canopy and biomass reduces the reflectivity value.

The physical properties of the seafloor determined from the acoustic backscatter, bottom samples, and underwater video imagery suggest that the water column environmental factors are affecting the lidar ability to detect the bottom in the shallow-water detection area. However, the dominant factors in deeper areas relate to the physical properties of the seafloor. The shallow-water detection area is distinct from the other two detection areas by its location in water depths of less than 7 m (Figs. 3 and 4). There is no correlation between the absolute slope values of the seafloor and the lidar ability to detect the bottom (Fig. 5). The slope range in shallow-water detection areas is 0°–23°, which is greater than, and overlaps, the lack-of-detection areas (0°–13°). The acoustic backscatter of the seafloor in both shallow-water detection area and lack-of-detection areas (Fig. 6) are similar, if not identical. This suggests that the dominant mechanism that affects the success of the ALB to detect the bottom in water shallower than 7 m is the water column environmental factor group independent of the seafloor environmental factor group. In areas deeper than 7 m, the dominant mechanism affecting the ability of the ALB to detect the bottom is the seafloor environmental factor group in addition to the water column environmental factor group.

Diffuse attenuation measurements at 532 nm from the UNH Coastal Ocean Observation Center archive on August 16, 2005 show that the average diffuse attenuation value was 0.2 m^{-1} ($K_d = 0.21$ m^{-1} and $K_{Lu} = 0.20$ m^{-1}). Although this is only a point measurement from one of the survey days, it suggests a relationship between the threshold and the two mechanisms that occurred at an optical depth $(K_d z)$ of 1.4. Knowledge of the attenuation coefficient may then allow a prediction of the threshold depth.

VI. Summary

Two ALB surveys were conducted in the western Gulf of Maine offshore Gerrish Island, Maine, USA in 2005. One survey was conducted according to NOAA survey standards that define a 3 m × 3 m spot spacing with a 200% overlap using a LADS MK-II system. The second survey was conducted according to USACE survey standards that define a 4 m × 4 m spot spacing with a 100% overlap using a SHOALS-3000 system. A bottom-detection pattern comparison of the two lidar surveys shows a striking correlation (95% overlap) of areas where no bottom detection was made from the lidar. This correlation is independent of the direction of flight or time of collection. Both lidar bathymetry data sets were compared to acoustic bathymetry that used a 300-kHz Kongsberg EM3002 multibeam echosounder. Three area groups were identified according to the laser measurements and water depth; areas shallower than 7 m that shows strong ALB bottom detection (shallow-water detection area), areas deeper than 7 m that show ALB bottom detection (deep-water detection areas), and areas

deeper than 7 m that show lack of bottom detection using ALB (lack-of-detection areas). The deep-water detection areas and the lack-of-detection areas are distinct from one another based on seafloor environmental factors. However, the results of this study did not show a correlation between the absolute slope values of the seafloor and the lidar ability to detect the bottom. Areas of bottom detection by lidar surveys correlate with low acoustic backscatter values, whereas the areas that lack bottom detection correlate with high acoustic backscatter values. It appears that there are two dominant mechanisms affecting the ability of ALB bottom detection. In the case study, the attenuated laser pulse in areas of water shallower than 7 m is strong enough to allow bottom detection independent of the seafloor characteristics. In areas where the water is deeper than 7 m, the laser pulse is reduced in energy by the water column properties and the laser bottom detection is dependent on the seafloor characteristics. In areas deeper than 7 m, there is a correlation between areas with sandy bottoms and the strong bottom detection by laser measurements and in areas with rocky bottoms, there is a correlation of ALB lack of bottom detection. An additional option that may affect lidar success to detect the seafloor in areas deeper than 7 m is a vegetated bottom (regardless of the bottom composition). The study results indicate that lack of bottom detection by ALB does not necessarily indicate water depths deeper than the surrounding areas with strong bottom detection by the lidar. Consequently, lack of detection could be misinterpreted to indicate deeper depths and may be a hazard to navigation.

ACKNOWLEDGMENT

The authors would like to thank Larry Mayer and Lloyd Huff from the University of New Hampshire, Adam Dunbar and Michael Askalsen from National Ocean Service, NOAA, David Scharff and Gerd Glang from Ocean Coastal Survey, NOAA, Joint Airborne Lidar Bathymetry Technical Center of Expertise (JALBTCX), and Fugro LADS for their numerous discussions. The authors acknowledge with appreciation the careful and constructive reviews given to this paper by Gary Guenther (Optech International). However, all the conclusions presented here are the authors' and do not necessarily represent those of the above reviewers.

REFERENCES

[1] G. C. Guenther, "Airborne lidar bathymetry," in *The DEM Users Manual, in Digital Elevation Model Technologies and Applications*, D. F. Maune, Ed., 2nd ed. Bethesda, MD: ASPRS, 2007, pp. 253–320.

[2] G. C. Guenther, "Airborne Laser Hydrography: System design and performance factors," NOS, NOAA, Rockville, MD, NOAA Prof. Paper Ser., Mar. 1985.

[3] E. J. Hochberg, A. Andrefouet, and M. R. Tyler, "Sea surface correction of high spatial resolution IKONOS images to improve bottom mapping in near-shore environments," *IEEE Trans. Geosci. Remote Sens.*, vol. 41, no. 7, pp. 1724–1729, Jul. 2003.

[4] W. D. Philpot, "Estimating atmospheric transmission and surface reflectance from a glint-contaminated spectral image," *IEEE Trans. Geosci. Remote Sens.*, vol. 45, no. 2, pp. 448–457, Feb. 2007.

[5] V. I. Feigels, B. Evans, L. Feygels, G. C. Guenther, and Y. Kopilevich, "Prediction of bathymetric lidar performance with Ocean Scientific 2001 simulation code," in *Proc. SPIE—Ocean Optics: Remote Sensing and Underwater Imaging*, R. J. Frouin and G. D. Gilbert, Eds., 2002, vol. 4488, pp. 61–70.

[6] R. M. Measures, *Laser Remote Sensing: Fundamentals and Applications*. Melbourne, FL: Krieger, 1992, 510 pp.

[7] C. D. Mobley, *Light and Water: Radiative Transfer in Neutral Waters*. New York: Academic, 2004. (CD version).

[8] G. H. Tuell and J. Y. Park, "Use of SHOALS bottom reflectance images to constrain the inversion of a hyperspectral radiative transfer model," in *Proc. SPIE—Laser Radar and Technology Applications IX*, G. Kammerman, Ed., 2004, vol. 5412, pp. 185–193.

[9] G. H. Tuell, V. Feygels, Y. Kopilevitch, A. D. Weidemann, A. G. Cunningham, R. Mani, V. Podoba, V. Ramnath, J. Y. Park, and J. Aitken, "Measurement of ocean water optical properties and seafloor reflectance with Scanning Hydrographic Operational Airborne Lidar Survey (SHOALS): II. Practical results and comparison with independent data," in *Proc. SPIE—Remote Sensing of the Coastal Oceanic Environment*, R. J. Frouin, M. Babin, and S. Sathyendranath, Eds., 2005, vol. 5885, p. 588 50D, DOI: 10.1117/12.619215.

[10] W. D. Philpot and C. K. Wang, "Using SHOALS LIDAR system to detect bottom material change," Hydrographic Sci. Res. Center, Univ. Southern Mississippi, Stennis Space Center, MS, 2004, Final Report, Agreement # USM-GR00662-07.

[11] G. R. Elston and S. J. Dijkstra, "Robust characterization of SHOALS lidar signals for bottom segmentation and classification: A combined parameter-estimation and curve-fitting approach," in *Proc. ASPRS Annu. Conf.*, Denver, CO, 2004.

[12] G. Tuell, J. Y. Park, J. Aitken, V. Ramnath, and V. Feygels, "Adding hyperspectral to CHARTS: Early results," in *Proc. U.S. Hydrographic Conf.*, San Diego, CA, 2005b.

[13] A. Collin, P. Archambault, and B. Long, "Mapping the shallow water seabed habitat with the SHOALS," *IEEE Trans. Geosci. Remote Sens.*, vol. 46, no. 10, pp. 2947–2955, Oct. 2008.

[14] J. C. Brock and S. J. Purkins, "The emerging role of lidar remote sensing in coral research and resource management," *J. Coast. Res.—SI*, vol. 53, pp. 1–5, 2009.

[15] S. J. Pittman, B. M. Costa, and T. Battista, "Using lidar bathymetry and boosted regression trees to predict the diversity and abundance of fish and corals," *J. Coast. Res.—SI*, vol. 53, pp. 16–26, 2009.

[16] G. C. Guenther and L. R. Goodman, "Laser applications for near-shore nautical charting," in *Proc. SPIE Ocean Opt. V*, 1978, vol. 160, pp. 174–183.

[17] V. I. Feygels and Y. I. Kopilevich, "Optimization of laser wavelength in oceanic lidars," *Proc. SPIE*, vol. 2964, pp. 128–137, 1996.

[18] M. F. Penny, R. H. Abbot, D. M. Phillips, B. Billard, D. Rees, D. W. Faulkner, D. G. Cartwright, B. Woodcock, G. J. Perry, P. J. Wilsen, T. R. Adams, and J. Richards, "Airborne laser hydrography in Australia," *Appl. Opt.*, vol. 25, no. 13, pp. 2046–2058, Jul. 1986.

[19] M. J. Sinclair and T. Spurling, "Operational laser bathymetry in Australia," in *Proc. XVth Int. Hydrographic Conf.*, Apr. 21–22, 1997, pp. 4.1–4.17, Session IV.

[20] R. A. Maffione and D. R. Dana, "In-situ characterization of optical backscattering and attenuation of lidar applications," *Proc. SPIE*, vol. 2964, pp. 152–162, 1996.

[21] Y. I. Kopilevich, V. I. Feygels, G. H. Tuell, and A. Surkov, "Measurement of ocean water optical properties and seafloor reflectance with scanning hydrographic operational airborne lidar survey (SHOALS): 1. Theoretical background," *Proc. SPIE*, vol. 5885, p. 588 50D, 2005.

[22] F. E. Hoge, R. N. Swift, and E. B. Frederick, "Water depth measurement using an airborne pulsed neon laser system," *Appl. Opt.*, vol. 19, no. 6, pp. 871–883, Mar. 1980.

[23] O. Steinvall, H. Klevebrant, J. Lexander, and A. Widen, "Laser depth sounding in the Baltic Sea," *Appl. Opt.*, vol. 20, no. 19, pp. 3284–3286, Oct. 1981.

[24] V. I. Feygels, Y. I. Kopilevich, A. Surkov, J. Yungel, and M. Behrenfeld, "Airborne lidar system with variable field-of-view receiver for water optical properties measurement," *Proc. SPIE*, vol. 5155, pp. 12–21, 2003.

[25] B. Collins, M. Penley, and X. Monteys, "Lidar seabed classification: New process for generation of seabed classes," *Hydro Int.*, vol. 11, no. 7, pp. 19–22, Jul./Aug. 2007.

[26] L. Fonseca and L. Mayer, "Remote estimation of surficial seafloor properties through the application Angular Range Analysis to multi-beam sonar data," *Mar. Geophys. Res.*, vol. 28, no. 2, pp. 119–126, Jun. 2007.

[27] P. M. Teillet, B. Guindon, and D. G. Goodenough, "On the slope-aspect correction of multispectral scanner data," *Can. J. Remote Sens.*, vol. 8, no. 2, pp. 84–106, 1982.

[28] P. Meyer, K. I. Itten, T. Kellenberger, S. Sandmeier, and R. Sandmeier, "Radiometric corrections of topographically induced effects on Landsat TM data in Alpine terrain," *ISPRS J. Photogramm. Remote Sens.*, vol. 48, no. 4, pp. 17–28, Aug. 1993.

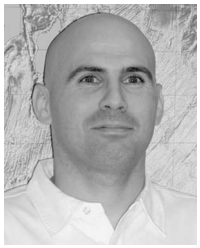

Shachak Pe'eri (M'07) received the B.Sc, M.Sc., and Ph.D. degrees in geophysics from the Tel Aviv University, Israel, Ramat Aviv, Israel, in 1996, 1997, and 2005, respectively.

He is currently working as a Research Assistant Professor with the Center of Coastal and Ocean Mapping, University of New Hampshire, Durham. His research activities have focused on experimental and theoretical studies of airborne lidar bathymetry and general optical remote sensing technologies for coastal studies.

James V. Gardner received the B.S. degree in geology from San Diego State University, San Diego, CA, in 1967 and the Ph.D. degree from Columbia University, New York, in 1973.

He is currently working as a Research Professor with the Center of Coastal and Ocean Mapping, University of New Hampshire, Durham. His focus is on marine sedimentology, paleoceanography, and seafloor mapping. In CCOM, he is in charge of the US Law of the Sea cruises as well as research methods to extract meaningful geological information from multibeam acoustic backscatter through ground truth and advanced image analysis methods.

Larry G. Ward received the Ph.D. degree in marine geology from the University of South Carolina, Columbia.

He is currently an Associate Research Professor with the Department of Earth Sciences and is a member of the Center for Coastal and Ocean Mapping and Jackson Estuarine Laboratory. His most recent research has focused on estuarine sedimentological processes and depositional environments, coastal geomorphology and erosion, the physical characteristics of inner shelf seafloor, and the stratigraphy, sea level history, and Holocene evolution of nearshore marine systems.

John Ru Morrison received the B.Sc. and Ph.D. degrees in marine biology and oceanography from the University of Wales, Bangor, Menai Bridge, U.K., in 1993 and 1999, respectively.

While writing this paper, he was an Assistant Research Professor with the Institute for the Study of Earth, Oceans, and Space at the University of New Hampshire. He is currently the Executive Director of the Northeastern Regional Association of Coastal Ocean Observing Systems (NERACOOS).